VERIZONA PUBLISHER
Publishing Your Ideas

www.verizonaonlinepublishing.com
Special Issue

Material Science and Engineering with Advanced Research

Al- (Al_9Co_2, $Al_{13}Co_4$) Powder Metallurgy Processed Composite Materials: Analysis of Microstructure, Sliding Wear and Aqueous Corrosion

G Bakoulis, AG Lekatou, A Poulia, AK Sfikas, K Lentzaris and AE Karantzalis*

Laboratory of Applied Metallurgy, Department of Materials Science & Engineering, University of Ioannina, 45110 Ioannina, Hellas

***Corresponding author:** AE Karantzalis, Laboratory of Applied Metallurgy, Department of Materials Science & Engineering, University of Ioannina, 45110 Ioannina, Hellas, Greece; Tel: (+30) 2651009026; Fax: (+30) 2651009082; E mail: akarantz@cc.uoi.gr

Article Type: Research, **Submission Date**: 09 February 2017, **Accepted Date:** 12 April 2017, **Published Date:** 15 June 2017.

Citation: G Bakoulis, AG Lekatou, A Poulia, AK Sfikas, K Lentzaris and AE Karantzalis (2017) Al- (Al_9Co_2, $Al_{13}Co_4$) Powder Metallurgy Processed Composite Materials: Analysis of Microstructure, Sliding Wear and Aqueous Corrosion. Mater. Sci. Eng. Adv. Res Special Issue: 52-59. doi: https://doi.org/10.24218/msear.2017.7S.

Abstract

The present effort was undertaken in order to investigate the manufacturing of aluminum based composites, reinforced by a dual intermetallic phase, Al_9Co_2 - $Al_{13}Co_4$, using a powder metallurgy route. The metal matrix was reinforced with compositions 2, 5 and 10% vol. The manufacturing of the dual Al_9Co_2 - $Al_{13}Co_4$ powders was carried out by vacuum arc melting followed by milling to produce fine-sized powders. The composite materials were produced by a common powder metallurgy route, including mixing in a mortar, consolidation by cold pressing, and sintering under vacuum at 600°C. The wear properties of the composite were examined by dry sliding wear against an alumina counter face at 10cm/s, a load at 1N and a distance at 1000m. Macro hardness was also assessed. Aqueous corrosion experiments in 3.5% NaCl at 25°C were carried out in all three different compositions. Optical microscopy and SEM-EDX analysis were used in order to ascertain the microstructure, the sliding wear tacks and debris and the corroded surfaces. The sliding wear phenomena were related to the microstructural features and approached based on classic theories of Al composite wear behaviour and so was the corrosion response of the produced materials.

Keywords: Al composites reinforced with Al_9Co_2 - $Al_{13}Co_4$, Vacuum arc melting, Powder metallurgy, Sliding wear, Aqueous corrosion.

Introduction

Aluminium Matrix Composites (AMCs) have gained intensive research interest during the last four decades, due to their improved mechanical and physical properties and have been considered as potential candidate materials for various, aerospace, automotive, structural and other civil and military applications [1-5]. Especially, AMCs have found application in the manufacture of various automotive and aerospace, engine or structural components such as cylinder blocks, pistons, piston insert rings, aircraft empennage, fuselage in fighter aircraft, rotary aircraft were dry sliding wear and corrosion resistance are predominant properties [6,7].

Various production methods for AMCs have been developed within these years, with the casting based processes being at the forefront due to the ease-to-handle operation scheme and, most importantly, their relatively low cost. Powder metallurgy, nevertheless, despite their relatively high cost, has attracted great attention in the manufacture of AMCs due to the unique properties these production routes may provide [1-5,8-12].

Many different reinforcing phases have been used in these materials, with oxides, borides and carbides being the most used. Intermetallic based compounds, however, have emerged in the scientific scheme as potential reinforcing phase due to their enhanced properties and especially due to the compatibility their metallic character may provide within the metallic Al matrix. The onset on the research of complex metallic alloys (CMA), gives rise to a totally new frontier in the use of intermetallics as potential reinforcing phases for AMCs [1-5].

The term CMA describes a new group of intermetallic compounds phases with giant unit cells (that contain at least a few tens of atoms) and lattice parameters of several nanometers [13].On the scale of several nanometers, the structure is crystalline with translational periodicity of the lattice; on the atomic scale, the atoms are arranged in clusters of polytetrahedral order, whilst they are distributed quasiperiodically [14]. The quasiperiodic order is considered responsible for unusual properties including amongst other unusual surface properties. The interesting surface properties (associated with a low surface energy) include low

wetting by water [15], low solid-solid adhesion [16,17], intriguing features in solid film growth [18]), oxidation resistance [18], corrosion resistance [19], friction anisotropy [20], low friction [16,18].Despite their unusual properties, CMA applications are still in an early stage of maturity. The reason is that being notably brittle, CMAs are regarded unsuitable for applications as monolithic alloys, but still viable as coatings and composites [19]. However, CMAs as coatings present intrinsically poor adherence to their substrates owing to their low surface energy [20]; thus, the use of a bond coat is recommended [21]. The production of two- or multi- phase structures including a soft metallic phase shows a large potential for improving the ductility of CMAs at low temperatures. So in order to examine the more promising, application oriented, use of CMAs as composite reinforcement phase, the current research was performed.

Sliding wear response is one of the most crucial issues, when trying to assess the overall behaviour of AMCs. It has been proved that, the mechanisms and phenomena related to the material loss during such kind of conditions are by far complicated issues that are related with the intrinsic characteristics (matrix type, reinforcement type, size and tape, interfacial reactivity etc.) and extrinsic parameters (load, counterbody, distance, speed etc.) without permitting as such, a unified material response theory [22-24]. Very little information can be found on the wear performance of Al-Co alloys. The most relevant information concerns the wear behavior of cast and rapidly solidified aluminum alloys in-situ reinforced by intermetallic compounds. In-situ particulate reinforcements of Al, such as Al_3Ti [25], (Al_2O_3+ $Ti(Al_{1-x},Fex)_3$) [26], TiB_2 [27], AlB_2 [28], ($Al_{12}W$+Al_5W+$Al_3(Ti,W)$) [29], Al_3Zr [30], ZrB_2[31], (ZrB_2+TiB_2) [32] have in general a positive contribution to the wear resistance of Al.

Aqueous corrosion behaviour of AMCs, on the other hand, is also related with numerous parameters of both the material system and testing conditions and also difficult to provide a solid well established mechanism. It has been postulated, however, that in the case of AMCs, if a clean and thermodynamically stable matrix-reinforcement interface is established, the aqueous corrosion behaviour is most likely dependent on the matrix corrosion characteristics rather than the presence of the reinforcing phase [33-40]. As for the corrosion behaviour of Co aluminides very limited information can be found. Palcut et al. [41,42], investigating the corrosion performance of Al-(24-29 at% Co) alloys consisting entirely of aluminides observed: a) three stages (an active corrosion stage, a very small stabilization stage and a steady current increase stage); b) galvanic coupling between nobler and less noble intermetallic phases and c) pitting in 0.6 mol/dm^3NaCl. Lekatou et al. [34] found that Al-(7-20 wt.%Co) alloys composed of various amounts of Al_9Co_2 in a (Al,Co) matrix exhibited low susceptibility to localized corrosion in 3.5 wt.% NaCl. Al-7 wt% Co showed a slightly higher corrosion resistance than the other compositions, in terms of corrosion rate, passivation current density and stress corrosion cracking indications.

Within the above framework, the corrosion and wear behavior of Al-CMA systems presents great research interest, especially when considering the issues: (i) the formation of two- or more phase structures based on a soft metallic phase shows the largest potential for improving the ductility of CMAs; (ii) CMAs are claimed to have excellent surface properties; (iii) aluminum alloys exhibit very poor tribological properties (aluminum being a light metal) and moderate resistance to aggressive environments [43]. On the above grounds, the present work investigates the manufacturing of aluminum based composites, reinforced by a dual intermetallic phase, Al_9Co_2 - $Al_{13}Co_4$, using a powder metallurgy route and examines their wear and corrosion resistance towards aggressive environments.

Experimental Procedure

Appropriate amounts, determined by the Al-Co phase diagram [44], of Al (<325 mesh) and Co powders (<40 μm) both by Sigma-Aldrich were weighted and mixed targeting the composition corresponding to the Al_9Co_2 intermetallic phase. Small loads (5g) of the mixture were mechanically pressed under 300 bar to form coupons that there were arc melted in an arc melting furnace (VAM) using W electrode at 120A current using Ar as protecting atmosphere. The resulting droplets were crushed and subjected to planetary ball milling for 10 minutes with the presence of alcohol. The resulting powder was dried and then mixed with appropriate amount of Al powder in order to produce 2, 5 and 10 vol.% in Al_9Co_2 composite materials respectively. Coupons of approximately 5g were formed by mechanical pressing under 250 bar and subjected to free sintering for 9h at 600°C under Ar atmosphere.

Specimens were metallographically prepared and examined under optical microscope (Leica 4000DM) and SEM-EDX (Jeol 6510 LV, x-Act Oxford Instruments). Sliding wear experiments were conducted using a CSM ball on disk tribometer, with 6mm Al_2O_3 ball as the counter-body, at 10 cm/s linear speed, 5mm rotation diameter, 20Hz acquisition time, 1N externally applied load and 1 km as overall sliding distance. The tests were interrupted every 200m for weighting the samples and record the resulting mass loss. Wear tracks and debris were also examined with SEM-EDX. Hardness measurements were conducted using a Universal Hardness Tester 700M by Innovatest.

Aqueous corrosion experiments were conducted in properly prepared samples using a Gill AC galvanostat by ACM Instruments, within a 3.5% NaCl solution, using an Ag/ AgCl/ 3.5 KCl reference electrode. The experiments were conducted keeping the solution pH at 7, at scanning rate of 10mV/min within the range of 1000 to 1500 mV after having ascertained the rest potential for 2h.

Results and Discussion

Microstructural observations

Figure 1 shows a panoramic view of the precursor Al-Co powder after vacuum arc melting and milling. It can be observed that the powder size lies within the range of approximately 1-50 μm. In the same Figure 1, the XRD analysis of the Al-Co intermetallic powder shows the existence of the Al_9Co_2 phase – as expected form the initial targeted composition – along with the presence of Al and $Al_{13}Co_4$. A possible solidification sequence for the precursor Al-Co powder may be as follows: (a) The high temperature achieved during arc melting ensures entire melting of the raw materials, (b) According to the Al–Co phase diagram, at ~1100°C, Al_3Co solidification starts. At 1093°C, peritectic reaction of the Al-rich liquid with Al_3Co occurs, leading to the formation of $Al_{13}Co_4$, (c) At 970°C, $Al_{13}Co_4$ peritectically reacts with molten Al to form Al_9Co_2 and (d) However, according to the Al–Co equilibrium phase diagram [44], the $Al_{13}Co_4$ phase should not exist at ambient temperatures. All the same, the high cooling rates during solidification following arc melting, do not allow for completion of the diffusion processes, and, consequently, attainment of an equilibrium state. Hence, the Al (l) + $Al_{13}Co_4$ = Al_9Co_2 peritectic reaction cannot run into completion, allowing the $Al_{13}Co_4$ phase to persist. Actually, its extensive presence at room temperature manifests the high cooling rates involved in the arc melting process adopted. To sum up, the formation of $Al_{13}Co_4$ is most likely attributed to the relatively high cooling rates during solidification after vacuum arc melting that most likely does not permit the $Al_{13}Co_4 \rightarrow Al_9Co_2$ transformation completion.

Figure 2 presents optical micrographs of the different produced composites. It can be observed that in all cases the microstructure is characterized by the uniform particle distribution either in the form of isolated particles or particle clusters. The existence of residual porosity is also evident. The microstructure of the produced materials is presented more clearly under SEM examination, as shown in Figure 3. The cross sections of the produced composites (Figure 3) reveal the uniform particle distribution. It is also evident the presence of particle clusters and residual porosity that both increase with increasing the

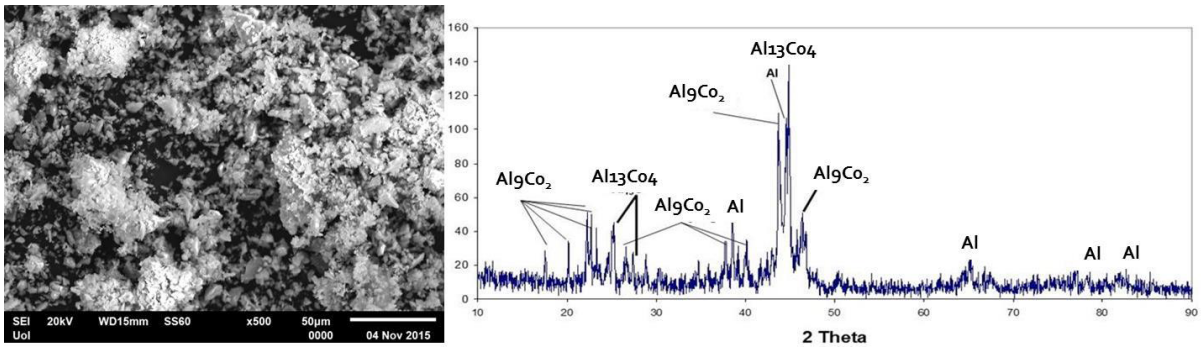

Figure 1: SEM micrograph showing the shape and size of the precursor Al-Co powder and XRD analysis showing the coexistence of both Al_9Co_2 and $Al_{13}Co_4$ phases

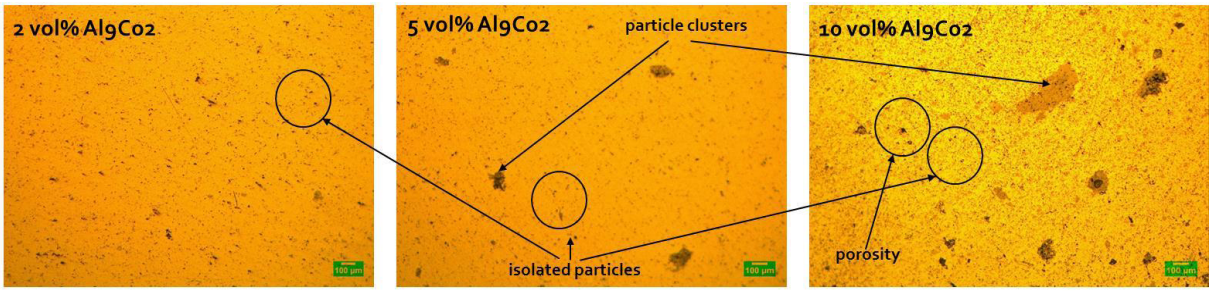

Figure 2: Optical micrographs showing the microstructure of the final composite materials

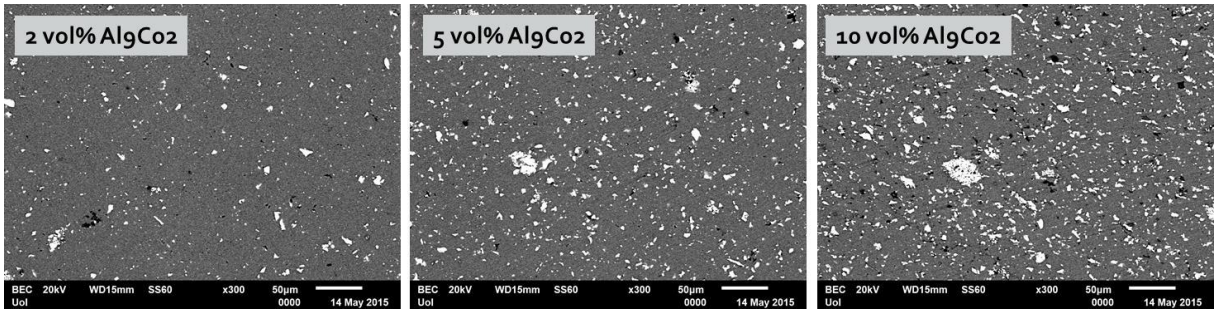

Figure 3: SEM images showing the cross sections of the produced materials, enlightening further their morphological features

reinforcement content. The clustering increase is most likely associated with primary particle clusters that did not disintegrate during the milling process. The increased porosity, on the other hand, maybe the result of either the observed particle clustering (particle clusters contain voids and gaps that can evolve into porosity upon processing) or insufficient sintering (the higher the reinforcing particles the more obstacles for their surrounding Al grains to get into intimate contact in order to promote and sustain effective sintering.

An interesting observation concerning the phase composition of the final composites arises from the elemental analysis on various reinforcing particles for all the different compositions, as presented in Figure 4. It can be seen that the Al-Co ratio in most of the cases, remains constant and practically corresponds to the Al_9Co_2 phase stoichiometry. Such observation, most likely suggests that upon the prolonged sintering conditions (600°C for 9h) allows the off equilibrium $Al_{13}Co_4$ phase to be fully transformed into Al_9Co_2 intermetallic compound.

Sliding wear behaviour

Figure 5 shows the volume loss as a function of the sliding distance for the different produced composites and their corresponding wear rates along with their hardness values. It can be observed that the wear rate is decreased with increasing the reinforcing particle content. It is also evident that the higher the particle content the higher the hardness value. These observations clearly verify the beneficial action of the reinforcing phase on the sliding wear resistance. Similar conclusions have been drawn by other researchers [24]. The wear resistance improvement is most likely associated with: a) the fact that reinforcing particles support the externally applied load, restricting in such way the intimate contact between the soft matrix and the counterbody which is responsible for the extreme plastic deformation and the resulting degradation phenomena, b) the provision of thermal, to the matrix stability, that postpones potential softening phenomena that promote severe plastic deformation and c) strain hardening effect due to particle dispersion strengthening effect that improves the matrix resistance to plastic deformation. All these potential improvement mechanisms are also well documented in other experimental works [22-24]. It has also to be mentioned that the wear response of the produced materials are in line with their hardness and the classic theory of Archard [45]: the higher

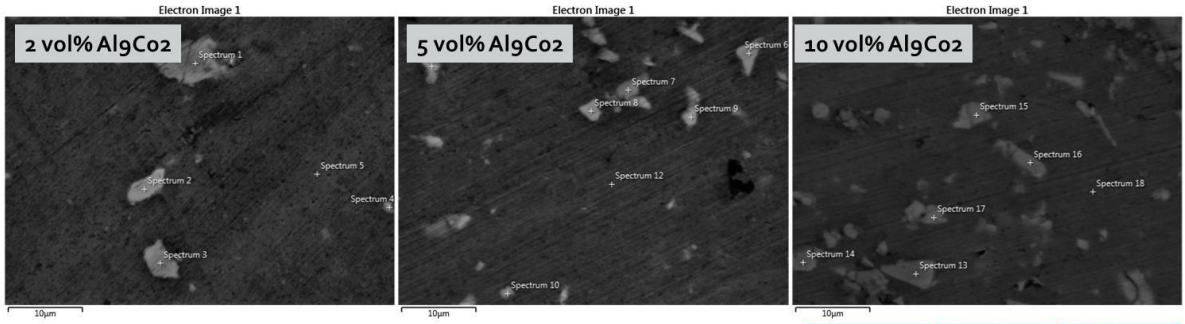

	Aluminium (Atomic %)	Cobalt (Atomic %)
Spectrum 1	83.13	16,78
Spectrum 2	84.27	15.73
Spectrum 3	85.46	14.54
Spectrum 4	95.59	4.41

	Aluminium (Atomic %)	Aluminium (Atomic %)
Spectrum 7	90.9	9.10
Spectrum 8	85.39	14.61
Spectrum 9	88.61	11.39
Spectrum 10	94.34	5.56

	Aluminium (Atomic %)	Cobalt (Atomic %)
Spectrum 13	83.39	16.61
Spectrum 14	84.50	15.50
Spectrum 15	89.55	10.45
Spectrum 16	86.78	13.22
Spectrum 17	88.93	11.07

Figure 4: Elemental analysis on various different reinforcing particles, reveling that the Al_9Co_2 phase prevails after the completion of the sintering process

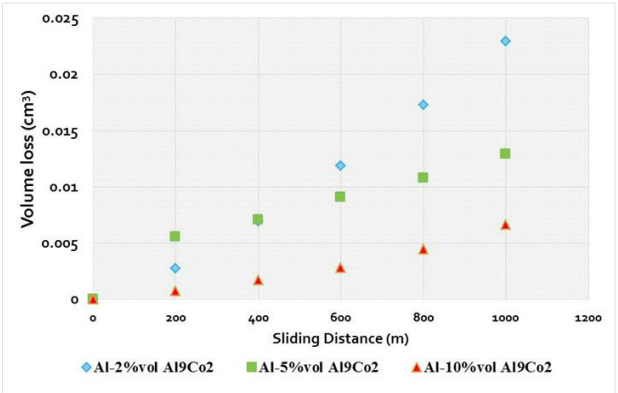

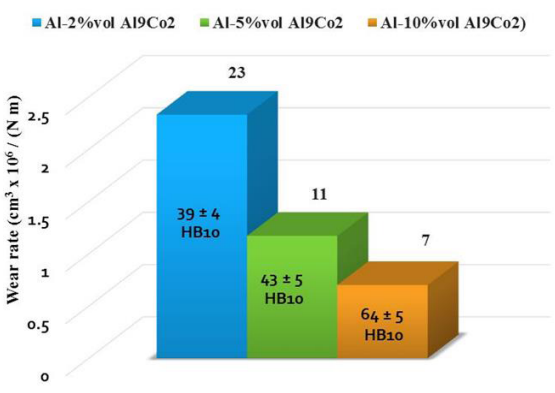

Figure 5: Volume loss vs sliding distance and corresponding wear rates of the produced materials

the hardness the higher the wear resistance.

A panoramic view of the wear track morphology of the produced composites is presented in Figure 6. It can be observed the characteristic "valley – hill" morphology – a result of the strain hardening effect of the soft matrix – which Sharkar [46] has explained in details the formation of and other research efforts also verified [24]. SEM-EDX point analysis reveals the presence of both oxide phases and cracks on the wear track surfaces. Both these features are responsible for the initiation and the promotion of the degradation phenomena which practically involves the development of cracks due to plastic deformation and or thermal fatigue on the oxide layer that eventually are promoted, expanded, bridged and lead to material loss [22-24].

The generated upon the sliding action debris is shown in Figure 7. This debris is also responsible for the wear phenomena especially for the slight abrasive action. It can be observed that the debris become finer and more equiaxed with the increase of sliding distance and the particle volume fraction. The sliding distance leads to prolonged surface oxide phases formation, which are brittle and are continuously entrapped at the counterfaces' gap and gradually fragmented into fine particles. The high particle content on the other hand increases the brittleness of the material, reducing its plasticity and leads to the formation of finer and more equiaxed debris [24].

Aqueous corrosion behaviour

Figure 8 shows the potentiodynamic polarization curves of the different produced materials and Figure 9 the forward polarization curves of these systems. Based on the data of these figures it can be postulated that: a) all the produced composites show a better behaviour to localized corrosion compared to

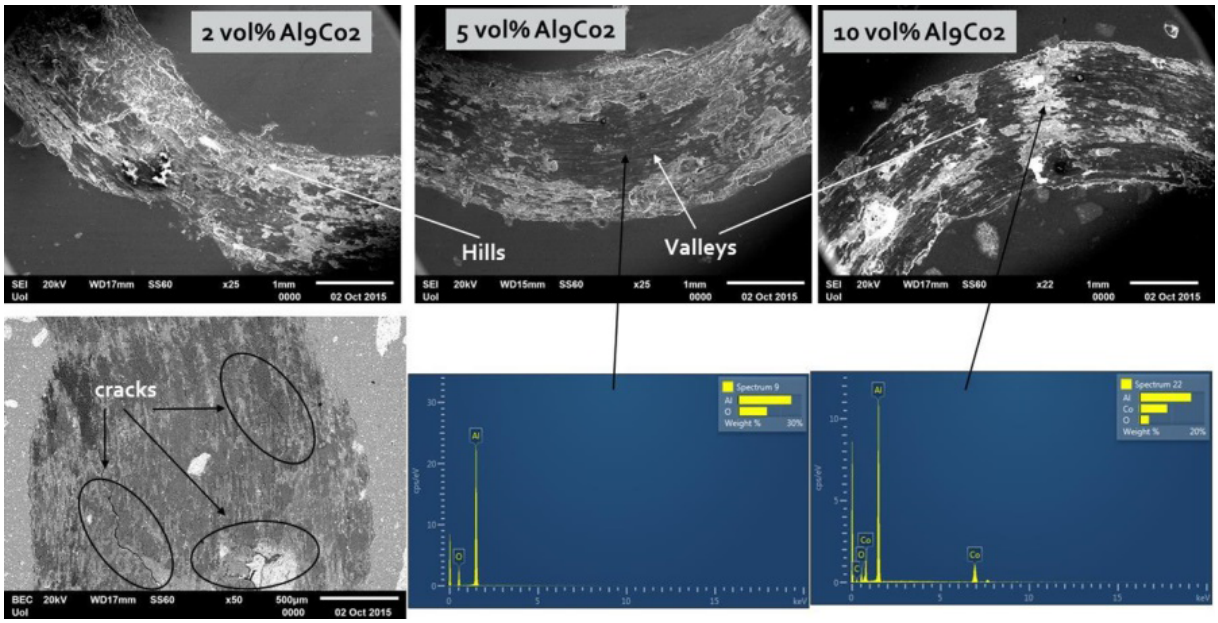

Figure 6: Panoramic view of the wear track morphology along with EDX analysis showing the presence of oxide phases.Crack formation is also evident

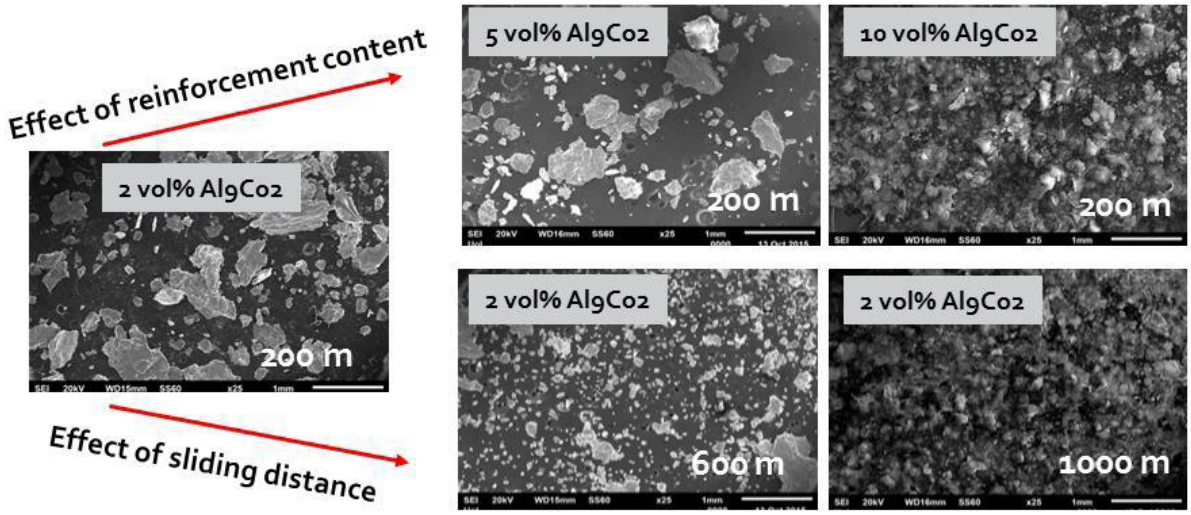

Figure 7: Debris morphology as a function of the distance and the reinforcing particle content

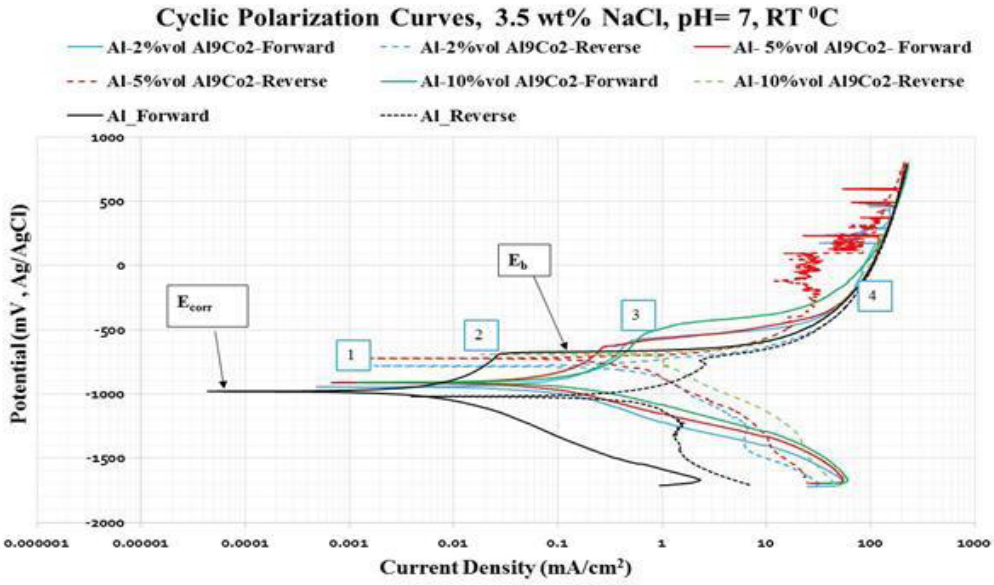

Figure 8: Potentiodyamic polarization curves of all the different materials tested

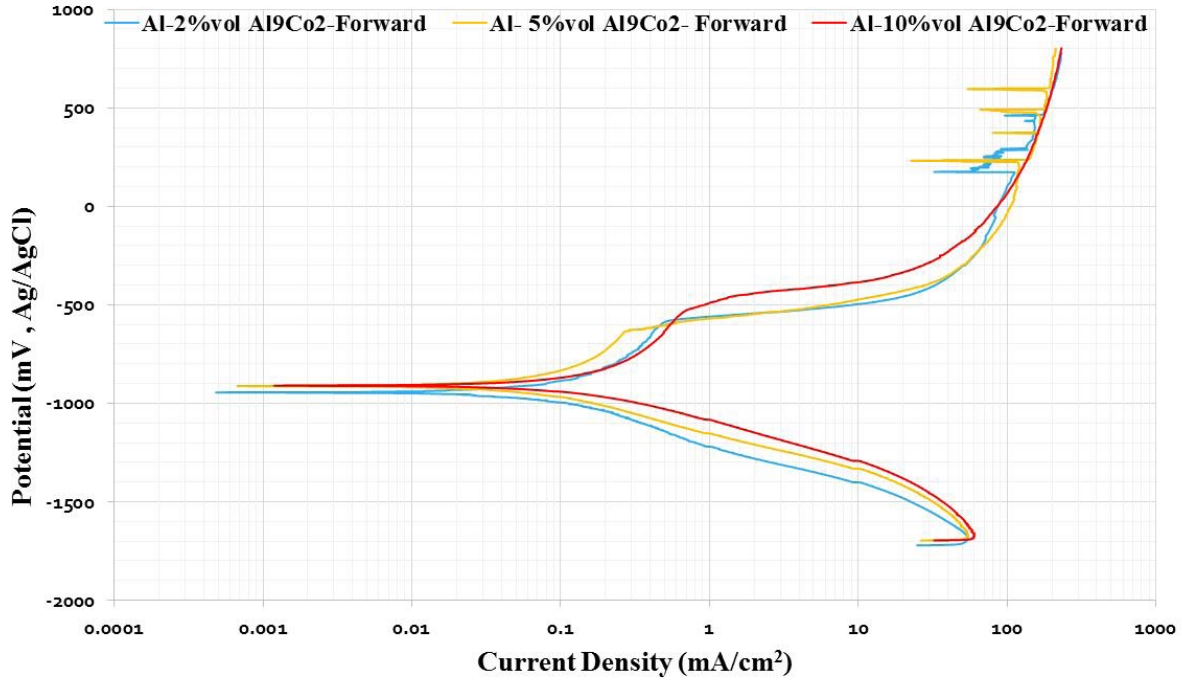

Figure 9: Forward potentiodynamic curves of the composite materials produced and tested

that of the monolithic Al alloy (breakdown potential (Eb) Al < Eb composite) with that of the 10 vol% system being the most optimum one as far the pitting corrosion resistance is concerned, b) after the energetic corrosion of stage 1, the monolithic alloy in stage 2 shows lower current densities compared to that of the composite materials due to the fact that the composite systems exhibit galvanic corrosion between the Al matrix and the Al_9Co_2 reinforcing phase and c) the steeper slopes of the composite materials in stages 3 and 4 is most likely a result of the greater extent of the mixed surface oxide phases consisting of Al and Co.

More specifically, in the case of the composite materials, in stage 2 the energetic corrosion is retarded due to the formation of either Al_2O_3 surface films of hydrated semiconducting Al(OOH) and $Al(OH)_3$ compounds. In stage 3, between the Al matrix and the Al_9Co_2 reinforcement, pitting corrosion takes place and in stage 4 a pseudo-passivation phenomenon can be observed as a result of possibly both the deposition of oxides and hydroxides within the pit cavities and/or the formation of mixed oxide and hydroxide phases of Al and Co. All these speculations are in agreement with previous research efforts [29,34,35].

Conclusions

Al – Al_9Co_2 based composites were successfully produced by a powder metallurgy based route. The particle distribution was

uniform with some degree of clustering and some porosity being observed, especially for the higher reinforcing particle concentrations.

Al_9Co_2 was identified as the only reinforcing phase due to the elimination of the primary $Al_{13}Co_4$ phase after the prolonged sintering stage.

Sliding wear resistance was increased with increasing the reinforcing particles volume fraction as did the hardness values, verifying the classic theories of aluminum metal matrix composites wear response. The familiar for these materials characteristic wear track landscape was also observed.

Aqueous corrosion experiments, showed that the composite systems have a better pitting corrosion resistance compared to that of the monolithic alloy with that of 10 vol.% reinforcing content, being the optimum one. A galvanic cell between the Al matrix and the nobler Al_9Co_2 is established and passivated at higher current densities.

The high sliding wear and localized corrosion resistance of the Al - 10 vol.% (Al_9Co_2, $Al_{13}Co_4$) constitute promising attribute for the future development of Al based composites with even higher reinforcement compositions, taking into account the desire for low weight, low cost of raw materials, high ductility and high fracture toughness.

Acknowledgements

Authors would like to thank Prof. Sofoklis Makridis who applied us part of the arc-melting apparatus system under his patent https://www.researchgate.net/publication/200664162_Multiapparatus_Arc_Melting_for_Rapid_Solidification_Processes?ev=prf_pub.

References

1. Lloyd DJ. Particle reinforced aluminium and magnesium matrix composites. International Materials Reviews. 1994; 39(1):1-23. doi: http://dx.doi.org/10.1179/imr.1994.39.1.1.
2. Rohatgi PK, Asthana R, Das S. Solidification, structures, and properties of cast metal-ceramic particle composites. International Materials Review. 1986; 31(1):115-139. doi: http://dx.doi.org/10.1179/imtr.1986.31.1.115.
3. Mortensen A, Jin I. Solidification processing of metal matrix composites, International Materials Review. 1992; 37(1):101-128. doi: http://dx.doi.org/10.1179/imr.1992.37.1.101.
4. Rohatgi PK, Ray S, Asthana R, Narendranath CS. Interfaces in cast metal-matrix composites. Materials Science and Engineering: A. 1993; 162(1-2):163-174. doi: http://dx.doi.org/10.1016/0921-5093(90)90041-Z.
5. Asthana R, Tewari SN. Interfacial and capillary phenomena in solidification processing of metal-matrix composites. Composites Manufacturing. 1993; 4(1):3-25. doi: http://dx.doi.org/10.1016/0956-7143(93)90012-W.
6. Deuis RL, Subramanian C, Yellup JM. Dry sliding wear of aluminium composites - A review. Composites Science and Technology. 1997; 57(4):415-435. doi: https://doi.org/10.1016/S0266-3538(96)00167-4.
7. Esakkiraj ES, Suresh S, Moorthi NSV, Kumar MK, Ranjith SMJ. Study of Mechanical Behaviour of Stir Cast Aluminium Based Composite Reinforced with Mechanically Ball Milled TiB_2 Nano Particles. Advanced Materials Research. 2014; 984-985:410-415. doi: https://doi.org/10.4028/www.scientific.net/AMR.984-985.410.
8. Liu YB, Lim SC, Lu L, Lai MO. Recent development in the fabrication of metal matrix-particulate composites using powder metallurgy techniques. Journal of Materials Science. 1994; 29(8):1999-2007. doi: http://dx.doi.org/10.1007/BF01154673.
9. Liu ZY, Wang QZ, Xiao BL, Ma ZT, Liu Y. Experimental and modeling investigation on SiC_p distribution in powder metallurgy processed SiC_p/2024 Al composites. Materials Science and Engineering: A. 2010; 527(21-22):5582-5591. doi: http://dx.doi.org/10.1016/j.msea.2010.05.006.
10. Pournaderi S, Mahdavi S, Akhlaghi F. Fabrication of Al/Al_2O_3 composites by in-situ powder metallurgy (IPM). Powder Technology. 2012; 229:276-284. doi: http://dx.doi.org/10.1016/j.powtec.2012.06.056.
11. Rahimian M, Parvin N, Ehsani N. The effect of production parameters on microstructure and wear resistance of powder metallurgy Al–Al_2O_3 composite. Materials and Design. 2011; 32(2):1031-1038. doi: http://dx.doi.org/10.1016/j.matdes.2010.07.016.
12. Rahimian M, Ehsani N, Parvin N, Baharvandi HR. The effect of particle size, sintering temperature and sintering time on the properties of Al–Al_2O_3 composites, made by powder metallurgy. Journal of Materials Processing Technology. 2009; 209(14):5387-5393. doi: http://dx.doi.org/10.1016/j.jmatprotec.2009.04.007.
13. Heggen M, Deng D, Feuerbacher M. Plastic deformation properties of the orthorhombic complex metallic alloy phase $Al_{13}Co_4$. Intermetallics. 2007; 15:1425-1431. doi: http://dx.doi.org/10.1016/j.intermet.2007.04.011.
14. Urban K, Feuerbacher M. Structurally complex alloy phases. Journal of Non-Crystalline Solids. 2004; 334–335:143–150. doi: http://dx.doi.org/10.1016/j.jnoncrysol.2003.11.029.
15. Dubois JM. A model of wetting on quasicrystals in ambient air. Journal of non-crystalline solids. 2004; 334-335:481–485. doi: http://dx.doi.org/10.1016/j.jnoncrysol.2003.12.041.
16. Dubois JM, Belin-Ferré E. Friction and solid-solid adhesion on complex metallic alloys. Science and Technology of Advanced Materials. 2014; 15(3). doi: https://doi.org/10.1088/1468-6996/15/3/034804.
17. Rabson DA. Toward theories of friction and adhesion on quasicrystals. Progress in Surface Science. 2012; 87(9-12):253–271. doi: http://dx.doi.org/10.1016/j.progsurf.2012.10.001.
18. Thiel PA. Quasicrystal Surfaces. Annual Review of Physical Chemistry. 2008; 59:129-152. doi: http://dx.doi.org/10.1146/annurev.physchem.59.032607.093736.
19. Eckert J, Scudino S, Stoica M, Kenzari S, Sales M. Mechanical engineering properties of CMAs. In: Dubois JM, Belin-Ferré E, editors. Complex Metallic Alloys: Fundamentals and Applications. Wiley-VCH; 2011. p. 273-315.
20. Polishchuk S, Boulet P, Mézin A, de Weerd MC, Weber S, Ledieu J, et al. Residual stress in as-deposited Al–Cu–Fe–B quasicrystalline thin films. Journal of Materials Research. 2012; 27(5):837-844. doi: https://doi.org/10.1557/jmr.2011.415.

21. Duguet T, Kenzari S, Demange V, Belmonte T, Dubois JM, FournéeV. Structurally complex metallic coatings in the Al-Cu system and their orientation relationships with an icosahedralquasi-crystal. Journal of Materials Research. 2010; 25(4):764-772. doi: https://doi.org/10.1557/JMR.2010.0101.

22. Sannino AP, Rack HJ. Dry sliding wear of discontinuously reinforced aluminum composites: review and discussion. Wear. 1995; 189(1-2):1-19. doi: http://dx.doi.org/10.1016/0043-1648(95)06657-8.

23. Deuis RL, Subramanian C, Yellup JM. Dry sliding wear of aluminium composites – a review. Composites Science and Technology. 1997; 57(4):415-435. doi: http://dx.doi.org/10.1016/S0266-3538(96)00167-4.

24. Mavros H, Karantzalis AE, Lekatou A. Solidification observations and sliding wear behavior of cast TiC particulate-reinforced AlMgSi matrix composites. Journal of Composite Materials. 2012; 47(17):2149-2162. doi: http://dx.doi.org/10.1177/0021998312454901.

25. Wu JM, Li ZZ. Contributions of the particle reinforcement to dry sliding wear resistance of rapidly solidified Al-Ti alloys. Wear. 2000; 244(1-2):147-153. doi: http://dx.doi.org/10.1016/S0043-1648(00)00452-X.

26. Hamid AA, Ghosh PK, Jain SC, Ray S. The influence of porosity and particles content on dry sliding wear of cast in situ Al(Ti)–Al_2O_3(TiO_2) composite. Wear. 2008; 265(1-2):14–26. doi: http://dx.doi.org/10.1016/j.wear.2007.08.018.

27. Kumar S, Chakraborty M, Sarma VS, Murty BS. Tensile and wear behaviour of in situ Al–7Si/TiB_2 particulate composites. Wear. 2008; 265(1-2):134–142. doi: http://dx.doi.org/10.1016/j.wear.2007.09.007.

28. Koksal S, Ficici F, Kayikci R, Savas O. Experimental optimization of dry sliding wear behavior of in situ AlB_2/Al composite based on Taguchi's method. Materials & Design. 2012; 42:124–130. doi: http://dx.doi.org/10.1016/j.matdes.2012.05.048.

29. Lekatou A, Karantzalis AE, Evangelou A, Gousia V, Kaptay G, Gácsi Z, et al. Aluminium reinforced by WC and TiC nanoparticles (ex-situ) and aluminide particles (in-situ): Microstructure, wear and corrosion behavior. Materials & Design. 2015; 65:1121–1135. doi: http://dx.doi.org/10.1016/j.matdes.2014.08.040.

30. Gautam G, Kumar N, Mohan A, Gautam RK, Mohan S. Tribology and surface topography of tri-aluminide reinforced composites. Tribology International. 2016; 97:49–58. doi: http://dx.doi.org/10.1016/j.triboint.2016.01.014.

31. Kumar N, Gautam G, Gautam RK, Mohan A, Mohan S. Wear, friction and profilometer studies of in-situ AA5052/ZrB_2 composites. Tribology International. 2016; 97:313–326. doi: http://dx.doi.org/10.1016/j.triboint.2016.01.036.

32. Rengasamy NV, Rajkumar M, Kumaran SS. Mining environment applications on Al 4032-Zrb_2 and Tib_2 in-situ composites. Journal of Alloys and Compounds. 2016; 658:757-773. doi: http://dx.doi.org/10.1016/j.jallcom.2015.10.257.

33. Gousia V, Tsioukis A, Lekatou A, Karantzalis AE. Al-MoSi_2Composite Materials: Analysis of Microstructure, Sliding Wear, Solid Particle Erosion, and Aqueous Corrosion. Journal of Materials Engineering and Performance. 2016; 25(8):3107-3120. doi: http://dx.doi.org/10.1007/s11665-016-1947-1.

34. Lekatou A, Sfikas AK, Petsa C, Karantzalis AE. Al-Co Alloys Prepared by Vacuum Arc Melting: Correlating Microstructure Evolution and Aqueous Corrosion Behavior with Co Content. Metals. 2016; 6(3):46. doi: http://dx.doi.org/10.3390/met6030046.

35. 35.Lekatou A, Sfikas AK, Karantzalis AE, Sioulas D. Microstructure and corrosion performance of Al-32%Co alloys. Corrosion Science. 2012; 63:193-209. doi: http://dx.doi.org/10.1016/j.corsci.2012.06.002.

36. McIntyre JF, Conrad PK, Golledge SL. The Effect of Heat Treatment on the Pitting Behavior of SiC_w/AA2124. Corrosion. 1990; 46(11):902-905. doi: http://dx.doi.org/10.5006/1.3580856.

37. Trzaskoma PP. Pit Morphology of Aluminum Alloy and Silicon Carbide/Aluminum Alloy Metal Matrix Composites. Corrosion. 1990; 46(5):402-409. doi: http://dx.doi.org/10.5006/1.3585124.

38. Trowsdale AJ, Noble B, Harris SJ, Gibbins ISR, Thompson GE, Woods GC. The influence of silicon carbide reinforcement on the pitting behavior of aluminum**.** Corrosion Science. 1996; 38(2):177–191. doi: http://dx.doi.org/10.1016/0010-938X(96)00098-4.

39. Tahamtan S, Halvaee A, Emamy M, Zabihi MS. Fabrication of Al/A206–Al_2O_3 nano/micro composite by combining ball milling and stir casting technology. Materials and Design. 2013; 49:347-359. doi: http://dx.doi.org/10.1016/j.matdes.2013.01.032.

40. De Salazar JMG, Urena A, Manzanedo S, Barrena MI. Corrosion behaviour of AA6061 and AA7005 reinforced with Al_2O_3 particles in aerated 3.5% chloride solutions: potentiodynamic measurements and microstructure evaluation. Corrosion Science. 1998; 41(3):529-545. doi: http://dx.doi.org/10.1016/S0010-938X(98)00135-8.

41. Palcut M, Priputen P, Kucy M, Janovec J. Corrosion behavior of Al-29at% Co alloy in aqueous NaCl. Corrosion Science. 2013; 75:461-466. doi: http://dx.doi.org/10.1016/j.corsci.2013.06.031.

42. Palcut M, Priputen P, Salgo K, Janovec J. Phase constitution and corrosion resistance of Al-Co alloys. Materials Chemistry and Physics. 2015; 166:95-104. doi: http://dx.doi.org/10.1016/j.matchemphys.2015.09.032.

43. Hollingsworth EH, Hunsicker HY. Corrosion of aluminium and aluminium alloys. In: Davis JR, editor. ASM Handbook, vol. 13: Corrosion, 9th ed. Materials Park, OH: ASM International; 1987. p. 583–609.

44. McAllister AJ. The Al-Co (Aluminum-Cobalt) system. Bulletin of Alloy Phase Diagrams. 1989; 10(6):646–650. doi: http://dx.doi.org/10.1007/BF02877635.

45. Archard JF. Contact and Rubbing of Flat Surfaces. Journal of Applied Physics. 1953; 24(8):981-988. doi: http://dx.doi.org/10.1063/1.1721448.

46. Sarkar AD. Friction and wear. Academic Press; 1980. p. 205-209.